DYNAMIC EXERGY ANALYSIS OF A RECUPERATIVE DUAL-PRESSURE ORC DRIVEN BY WASTE HEAT

Nan Jiang[1], Yang Du[1,2], Kang Cheng[1], Gang Fan[1], Jiangfeng Wang[1], Pan Zhao[1], Yiping Dai[1]*

[1] Institute of Turbomachinery, School of Energy and Power Engineering,
Xi'an Jiaotong University, Xi'an, Shaanxi 710049, China

[2] Department of Energy Conversion and Storage, Technical University of Denmark, Roskilde DK-4000, Denmark

*Corresponding Author: ypdai@mail.xjtu.edu.cn

ABSTRACT

To absorb the waste heat from low-temperature heat source more effectively, an ORC system is proposed. Compared with the traditional ORC system, an evaporator and a recuperator is added to the cycle. It is driven by the waste heat of solid bulk, R1234ze(E) is chosen as the working fluid. To study the dynamic characteristics of the system, disturbance is applied to the hot air inlet temperature. The results indicate that under 10℃ step decrease of hot air inlet temperature, the exergy efficiency of three heat exchangers all rises to the peak first, and then gradually declines. Compared with the initial state, the exergy efficiency of the high-pressure evaporator (HPE) increases the most in the end, which is 1.07%. Both high-pressure evaporator and low-pressure evaporator (LPE) take 700 seconds to return to steady state, while the recuperator only takes about 200 seconds. The exergy efficiencies of turbine, HPE and LPE drop directly when the disturbance occurs. The turbine exergy efficiency has a decline of 0.52%, from 81.1% to 80.58%. The system exergy efficiency firstly jumps from 35.67% to 43.28% and then slowly decreases to 34.65%.

Key words: dual-pressure ORC; exergy efficiency; dynamic analysis; finite volume method.

1 INTRODUCTION

Nowadays, the world is faced with a series of crisis caused by the shortage of energy and global warming (Imran 2018). In order to alleviate and even solve this key problem related to the future survival of mankind, people begin to explore how to use energy more efficiently. The effective utilization of low-temperature heat sources has attracted more and more attention in recent years. Low-temperature heat sources generally refer to heat sources with a temperature below 200°C, accounting for 50% of the total global heat generation, which can be formally divided into natural heat (such as geothermal, solar, biomass) and industrial waste heat (Lee 2020). However, compared with heat sources in medium or high temperature, low-temperature heat sources are more difficult to be utilized effectively. That is because the traditional steam Rankine cycle cannot work normally under low pressure and temperature working fluid conditions (Ravi 2018). Therefore, people changed the working fluid in the traditional Rankine cycle from water to organic working fluids. With a lower boiling point, the working fluid can generate higher pressure so that it can absorb low-temperature heat source more effectively. Such cycle is called organic Rankine cycle (ORC).

The evaluation of the system based on the first and second laws of thermodynamics is an important part of the research on the organic Rankine cycle. Wan et al. (2019) built a geothermal-solar flash-binary hybrid power generation system, which is composed of a top ORC system and a bottom ORC system. The system power can reach 12.76MW, the thermal efficiency is 10.74%, and the exergy efficiency is 23.9%. Zhi et al. (2019) proposed a new transcritical-subcritical parallel ORC system. This system was compared with a dual-loop ORC system and a parallel ORC. It is found that its maximum output power is increased by 12.02%. Jafary et al. (2020) compared the thermal efficiency and exergy efficiency of two new ORC systems. It is found that the system with internal heat exchanger has a higher overall energy efficiency and exergy efficiency. Hou et al. (2020) conducted a thermodynamic analysis and

optimization of a solar ORC system equipped with a compound parabolic collector. After optimization, the average system net power output and exergy efficiency can reach 143.02kw and 7.75% respectively. Compared with the traditional ORC, a new type of dual-pressure ORC (DORC) has appeared in recent years. Since the dual-pressure ORC has more parameters to optimize, it can effectively reduce the exergy loss of the heat exchanger. As a result, the exergy efficiency of the system can be improved (Li et al. 2018). Li et al. (2019) used the second law of thermodynamics to analyze the exergy efficiency of the dual-pressure ORC which uses azeotropic working fluid. Sun et al. (2020) found that for dual-pressure ORC, the inlet pressure of evaporators has a certain value to achieve the best system performance, and increasing inlet parameters of evaporators will also help improve the system performance.

In addition to using the first and second laws of thermodynamics to analyze the performance of ORC, research has also been carried out on the dynamic characteristics of ORC. Lin et al. (2019) conducted a dynamic analysis of the ORC system used in automobile internal combustion engines and found that compared with ordinary ORC, ORC with oil storage circuits has stronger stability and heat recovery performance in the face of fluctuations in heat sources, and the decrease in system output power is also lower. Manuel et al. (2017) analyzed the influence of the evaporator geometry and material selection on the dynamic response characteristics of the ORC system. The results show that response time can be used as a reference for evaporator selection and design. Ni et al. (2018) analyzed the dynamic response characteristics of the ORC system driven by solar energy in the face of cloud interference. It shows that short-term cloud cover to the sun has no obvious influence on the system. Chen et al. (2019) developed an improved model of ORC system. It is found that when different disturbances are applied to the system, the specific enthalpy of the working fluid at the outlet of the evaporator will have an abnormal change suddenly. Yu et al. (2021) made a research on the dynamic behavior of ORC under fluctuating heat source conditions. The result shows that an amplitude of 25~40K is acceptable to ensure the high efficiency of the system.

Although many researches have been done on the ORC system, most of them only focus on the analysis of steady-state systems. The analysis of the dynamic response of the system mostly focuses on the overall performance changes. More attention should be paid on the dynamic thermodynamic performance changes. In this article, a recuperative dual-pressure ORC system which uses the waste heat of solid bulk has been built and we stepped down the environment temperature by 10°C. Based on the system, the exergy analysis of each component has been conducted and research on their exergy efficiency changes has been done.

2 Description of system

The system diagram of a recuperative dual-pressure organic Rankine cycle (RDORC) is shown as Figure 1.

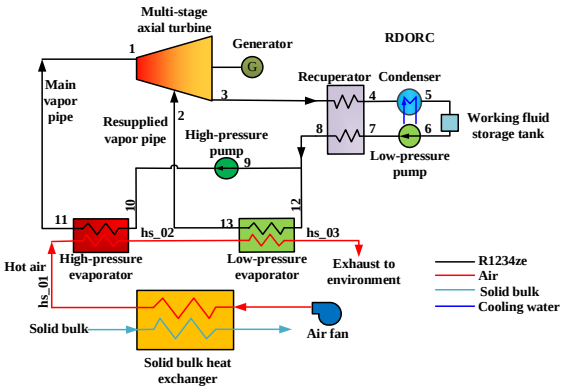

Figure 1: Diagram of RDORC driven by solid bulk waste heat using air as heat transfer medium

It is driven by the waste heat of solid bulk. The air fan pumps the air into the solid bulk heat exchanger. After absorbing the heat from the solid bulk, the hot air enters the high-pressure evaporator (HPE) and the low-pressure evaporator (LPE) in turn to heat the working fluid R1234ze(E) that drives the operation of the ORC system, and then discharges to the atmosphere. The heated R1234ze(E) from HPE enters

the high-pressure stage of the turbine, while the working fluid from LPE enters the low-pressure stage. After driving the turbine to work, working fluid enters the condenser and turns into saturated liquid. After being pressurized by the low-pressure pump (LPP), working fluid then divides into two shares. One enters the LPE directly, the other is pumped into the HPE by the high-pressure pump (HPP).

3 Dynamic modelling

3.1 Tube-and-shell heat exchanger model

Figure 2 shows the dynamic model of the tube-and-shell heat exchanger. It is divided into three parts, which are shell side, metal wall and shell side. The hot fluid flows in the shell side, while the cold fluid flows in the tube side. The heat exchanger is also divided into n volumes of the same size, length of which is Δx. That is because the finite volume method is adopted. Compared with moving boundary method, the finite volume method can get more accurate results. In order to construct the conservation equation for each discrete volume, the lumped parameter method is applied.

The finite volume method is applied to the tube-and-shell heat exchanger dynamic modelling due to its better accuracy compared with moving boundary method, as shown in Figure 2.

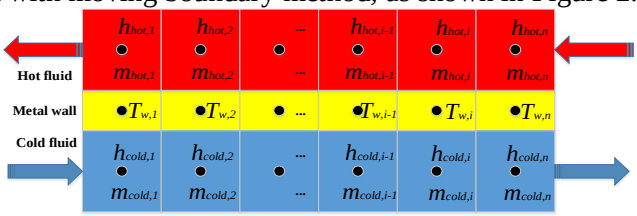

Figure 2: Finite volume method for tube-and-shell heat exchanger

For the i^{th} part of the cold fluid, the mass conservation equation is shown as

$$m_{cold,i\text{-}1} - m_{cold,i} = V_{cold,i}\frac{\partial \rho_{cold,i}}{\partial \tau} \tag{1}$$

In terms of conservation of energy, it can be obtained by the following equation:

$$Q_{conv,cold,i} + m_{cold,i\text{-}1}h_{cold,i\text{-}1} - m_{cold,i}h_{cold,i} = V_{cold,i}\frac{\partial\left(\rho_{cold,i}h_{cold,i} - p_{cold}\right)}{\partial \tau} \tag{2}$$

In the equation above, Q_{conv} is the convective heat transfer rate between cold side and wall. It is defined as:

$$Q_{conv,cold,i} = \alpha_{cold,i}A_{cold,i}(T_{w,i} - T_{cold,i}) \tag{3}$$

Metal wall is between hot fluid and cold fluid, its energy conservation can be defined as

$$Q_{conv,hot,i} - Q_{conv,cold,i} + Q_{cond,i} = \rho_w V_{w,i} c_{p,w}\frac{\partial T_{w,i}}{\partial \tau} \tag{4}$$

where Q_{cond} means the conductive heat transfer rate along the axis between each cell of the metal wall. It can be calculated by the following equation:

$$Q_{cond,i} = -\lambda_w\left(\frac{T_{w,i} - T_{w,i-1}}{\Delta x} + \frac{T_{w,i} - T_{w,i+1}}{\Delta x}\right)\frac{\pi(d_i^2 - d_o^2)}{4} \tag{5}$$

The energy conservation equation of hot fluid is similar to that of cold side. The difference is that, hot fluid loses heat while cold fluid gets heat.

$$m_{hot,i}h_{hot,i} - m_{hot,i-1}h_{hot,i-1} - Q_{conv,hot,i} = V_{hot,i}\frac{\partial\left(\rho_{hot,i}h_{hot,i} - p_{hot}\right)}{\partial \tau} \tag{6}$$

Just like cold fluid, Q_{conv} between hot fluid and wall can be obtained by

$$Q_{conv,hot,i} = \alpha_{hot,i}A_{hot,i}(T_{hot,i} - T_{w,i}) \tag{7}$$

3.2 Turbine model

Figure 3 shows the h-s diagram of the turbine in RDORC. Since the turbine has two stages, there are two work processes in the diagram. The working fluid absorbs the heat from the HPE. Then it enters the high-pressure stage of the turbine. In the high-pressure stage, R1234ze(E) is heated and expanded to state point 2a. It is then mixed with the organic vapor from the LPE (state point 2). The mixed vapor reaches 2b point, then it expands to work in the low-pressure stage of the turbine. Finally, it reaches point 3 and is discharged from the turbine.

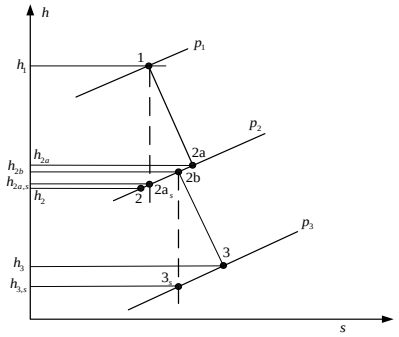

Figure 3: h-s diagrams of multi-stage turbine in RDORC

The enthalpy of the mixed steam at the inlet of the low-pressure stage is defined by

$$h_{2b} = \frac{m_1 h_{2a} + m_2 h_2}{m_1 + m_2} \tag{8}$$

The output power of the turbine is given by the following formula

$$W_{tur} = m_1 (h_1 - h_{2a,s}) \eta_{tur,high} + (m_1 + m_2)(h_{2b} - h_{3,s}) \eta_{tur,low} \tag{9}$$

The rated efficiency of the HPP and the LPP is set to 0.7. Under dynamic conditions, the speed of the HPP and the LPP can be adjusted to match different pressure heads. The relationship between volumetric flow rate, pressure head and speed satisfies the following equation:

$$\frac{q}{q_{des}} = \frac{N}{N_{des}} \tag{10}$$

$$\frac{H}{H_{des}} = \left(\frac{N}{N_{des}} \right)^2 \tag{11}$$

3.3 Pump model

In the recuperative dual-pressure ORC system, the design working speed of HPP and LPP is set as 1500rpm. The power consumption of the pump is defined as:

$$W_{pum,high} = \frac{m_{pum,high} \Delta h_{s,pum,high}}{\eta_{pum,high}} \tag{12}$$

$$W_{pum,low} = \frac{m_{pum,low} \Delta h_{s,pum,low}}{\eta_{pum,low}} \tag{13}$$

Pump efficiency under dynamic conditions is defined as:

$$\frac{1-\eta_{pum}}{1-\eta_{pum,des}} = \left(\frac{N_{des}}{N} \right)^{0.07} \tag{14}$$

3.4 Compressible pipe vapor volume

The compressible pipeline volume 1 is located between the outlet of the HPE and the inlet of the high-pressure stage of the steam turbine. Volume 2 is located between the outlet of the LPE and the inlet of the low-pressure stage of the steam turbine. It is assumed that there is no energy loss to the outside in the compressible pipe volume. The purpose of the establishment of this model is to obtain the evaporation pressure of the two evaporators located downstream. In order to obtain the evaporation pressure, the mass conservation equation, the energy conservation equation and the ideal gas law are utilized to obtain the organic vapor mass M_{vap}, the average vapor temperature T_{vap}, and the average compressible volume pressure p_{eva}.

$$m_{in,pipe} - m_{out,pipe} = \frac{\partial M_{vap,pipe}}{\partial \tau} \tag{15}$$

$$u_{vap,pipe}\frac{\partial M_{vap,pipe}}{\partial \tau} + M_{vap,pipe}c_v\frac{\partial T_{vap,pipe}}{\partial \tau} = m_{in,pipe}h_{in,pipe} - m_{out,pipe}h_{out,pipe} \tag{16}$$

$$\frac{RT_{vap,pipe}}{V_{vap,pipe}}\frac{\partial M_{vap,pipe}}{\partial \tau} + \frac{p_{eva}}{T_{vap,pipe}}\frac{\partial T_{vap,pipe}}{\partial \tau} - \frac{\partial p_{eva}}{\partial \tau} = 0 \tag{17}$$

3.5 Mathematical model of exergy analysis

In this study, exergy efficiency is selected to analyze the transient characteristics of RDORC. To evaluate the dynamic characteristics of the system better, exergy is divided into chemistry exergy and physics exergy.

$$E = E_{phy} + E_{che} \tag{18}$$

In the process of exergy analysis, conservation of mass, conservation of energy and conservation of exergy are introduced:

$$\sum m_{in} = \sum m_{out} \tag{19}$$

$$Q - P = \sum m_{out}h_{out} - \sum m_{in}h_{in} \tag{20}$$

$$\sum E_{in} + \sum E_{Q} = \sum E_{out} + P + \sum I \tag{21}$$

Table 1 shows the formulas for calculating the exergy efficiency of the main components.

Table 1: Exergy efficiency of components in RDORC

HPE	$\eta = \frac{m_1(h_{10} - h_{11} - T_0(s_{10} - s_{11}))}{m_{hs}(h_{hs\_01} - h_{hs\_02} - T_0(s_{hs\_01} - s_{hs\_02}))}$	(22)
LPE	$\eta = \frac{m_1(h_{13} - h_{12} - T_0(s_{13} - s_{12}))}{m_{hs}(h_{hs\_02} - h_{hs\_03} - T_0(s_{hs\_02} - s_{hs\_03}))}$	(23)
Recuperator	$\eta = \frac{m_3(h_8 - h_7 - T_0(s_8 - s_7))}{m_3(h_3 - h_4 - T_0(s_3 - s_4))}$	(24)
HPP	$\eta = \frac{m_9(h_{10} - h_9 - T_0(s_{10} - s_9))}{W_{HPP}}$	(25)
LPP	$\eta = \frac{m_6(h_7 - h_6 - T_0(s_7 - s_6))}{W_{LPP}}$	(26)
Turbine	$\eta = \frac{W_{HPT} + W_{LPT}}{m_1h_1 + m_2h_2 - m_3h_3 - T_0(m_1s_1 + m_2s_2 - m_3s_3)}$	(27)

where subscript HPT means high pressure turbine, LPT means low pressure turbine.

4 Results and discussion

4.1 Design parameters of RDORC

To make the system get the maximin exergy efficiency, the genetic algorithm is utilized to optimize the initial parameters of each state points in the RDORC system. The value of the system under design conditions is given in Table 2. The nominal power output of this RDORC system is 27.11kW. The specific statics is shown in the Table 3, which includes mass flow, temperature and pressure.

Table 2: The design parameters of RDORC

System design parameters	Design value
Heat source temperature	393.15K
Heat source flow	5.388kg/s
Temperature difference of high-pressure evaporator	5.0K
Temperature difference of low-pressure evaporator	5.0K
System thermal efficiency	7.65%
High-pressure pump isentropic efficiency	70%
Low-pressure pump isentropic efficiency	70%
High-pressure stage isentropic efficiency	80%
Low-pressure stage isentropic efficiency	80%

Table 3: Initial design parameters of each state points in RDORC

State point	Mass flux (kg/s)	Temperature (℃)	Pressure (kPa)
1	1.3013	87.93	2137
2	0.6394	52.1	926
3	1.9407	40.88	578
4	1.9407	35.27	578
5	1.9407	30	578
6	1.9407	30	578
7	1.9407	30.29	926
8	1.9407	34.3	926
9	1.3013	34.3	926
10	1.3013	35.34	2137
11	1.3013	87.93	2137
12	0.6394	34.3	926
13	0.6394	52.1	926
hs_01	5.388	120	120
hs_02	5.388	75.2	120
hs_03	5.388	54.92	120

The geometric parameters of heat exchangers in RDORC is quite important to build the system and complete the simulation. Among the many geometric parameters, the heat exchange area of the heat exchanger is one of the main factors. Table 4 shows the specific values of the heat exchange area of each heat exchanger.

Table 4: Design heat exchanger parameters of RDORC

Item	HPE	LPE	Recuperator	Condenser
Heat transfer area (m^2)	178.95	79.42	22.62	53.59

4.2 Dynamic exergy performance to a 10℃ step decrease of hot air inlet temperature

A 10℃ step decrease of hot air inlet temperature is imposed on the RDORC system. Figure 4 shows the curve of the system's exergy efficiency. When the disturbance occurs, the exergy efficiency of the system jumps from 35.67% to 43.28%. Then the efficiency gradually declines from the peak. After the disturbance of 700 seconds, the exergy efficiency arrives at the steady state. Finally, the exergy efficiency reduces to 34.65%, which is 1.02% lower than the initial value. Figure 5 indicates the exergy efficiency of HPE. When the inlet temperature of hot air drops 10℃ at 100_{th} second, the dynamic exergy efficiency of HPE jumps from 73.85% to 98.23%. Then it gradually declines and reaches steady state at 800_{th} second. The steady-state exergy efficiency is 74.92%, which is 1.07% higher than the initial-state exergy efficiency.

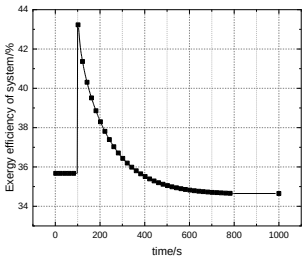

Figure 4: The exergy efficiency of system

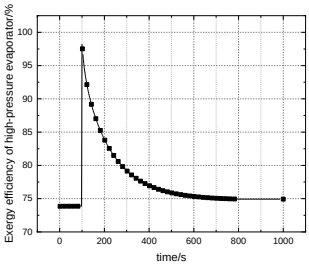

Figure 5: The exergy efficiency of HPE

As shown in Figure 6, the curve of the exergy efficiency of LPE is similar to that of HPE. The difference is that when the temperature drops, the exergy efficiency first jumps from 62.34% to 66%, then it suddenly drops to 64.86%. After that, the efficiency quickly rises to 65.8%, then it drops slowly and reaches the steady state at about 800_{th} second. Just like HPE, the exergy efficiency in the end, which is 62.48%, is also higher than that of the initial state. Figure 7 shows the exergy efficiency of the recuperator. The exergy efficiency jumps to 85.58% as soon as the temperature declines 10℃, then it declines quickly to the stable state. It costs about 200 seconds to reach a fixed value, which is 70.22%. Compared with HPE and LPE, recuperator has a better ability to recover from external disturbance. The exergy efficiency at last is slightly higher than the beginning value.

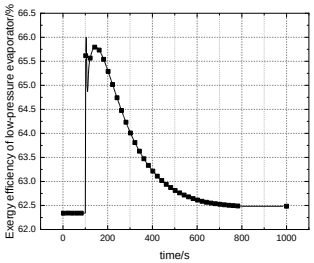

Figure 6: The exergy efficiency of LPE

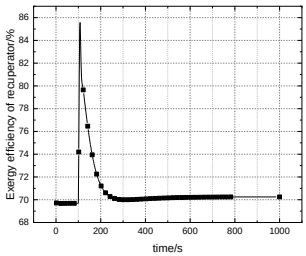

Figure 7: The exergy efficiency of recuperator

Figure 8-10 show the exergy efficiency of HPP, LPP and turbine successively. All of them have similar trends. When the temperature drops, the exergy efficiency of all three declines a little in a step. Then the exergy efficiency begins to decline gradually until 800_{th} second. At 800_{th} second, all of them reaches the steady state. For HPP, the beginning exergy efficiency is 71.47%, and the final state is 70.43%. For LPP, the initial exergy efficiency is 71.01%, the final exergy efficiency is 70.2%. For the turbine, the exergy efficiency drops from 81.1% to 80.58%. The exergy efficiency of HPP has the largest drop, which is 1.04%. While that of turbine has the smallest drop, which is 0.52%.

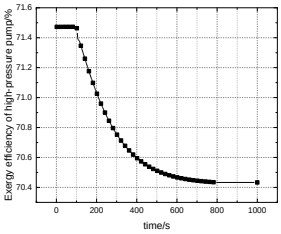

Figure 8: The exergy efficiency of HPP

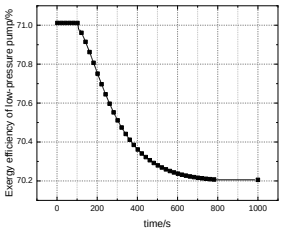

Figure 9: The exergy efficiency of LPP

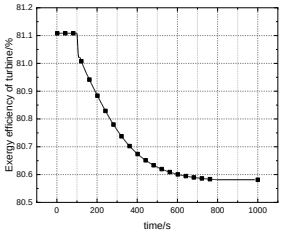

Figure 10: The exergy efficiency of turbine

4.3 Discussion

Under 10℃ step decrease of T_{hs_01}, the exergy efficiency of the system first jumps to the peak, then it gradually declines to the steady state. Compared with the initial state, it drops by 1.02%. All the three heat exchangers have a sharp increasement in exergy efficiency. Then, the exergy efficiency of high-pressure evaporator (HPE) and recuperator gradually decline until they reach the steady state. While the exergy efficiency of low-pressure evaporator (LPE) declines quickly after the surge, then it increases again and begins to decrease at 146_{th} second. Compared with HPE and LPE, the exergy efficiency of recuperator returns to the steady state in a shorter time, which is 200 seconds. While the exergy efficiency of HPE and LPE spends about 800 seconds to return to steady state. From the final state to the initial state, the exergy efficiency of HPE increases the most among three heat exchangers, which is 1.07%. While that of LPE increases the least, which is 0.14%. When the T_{hs_01} drops by 10℃, the exergy efficiency of high-pressure pump (HPP), low-pressure pump (LPP) and turbine has a similar trend. As the external disturbance happens, the exergy efficiency of them has a little step drop. Then it begins to decline gradually and finally keeps constant. It takes about 700 seconds for all of them to become stable. During the process, the turbine has the smallest drop, which is 0.52%. While HPP has the largest drop, which is 1.04%.

Since the temperature of the heat source has a step drop of 10℃, the temperature difference on two sides of the heat exchanger is correspondingly reduced. The sudden change of the heat source temperature makes the isentropic efficiency change rapidly. The isentropic efficiency of three heat exchangers decreases sharply, which makes entropy generation increase a lot. The sudden jump of entropy generation leads to a corresponding sudden increase in exergy efficiency. After the disturbance's occurrence, the isentropic efficiency of three heat exchangers returns to the original value. As a result, the exergy efficiency decreases gradually to the steady state. As the temperature gradient is reduced, the irreversibility rates reduce accordingly. As a result, the exergy efficiency of the three heat exchangers is slightly improved after the system returns to the steady state. For two pumps and the turbine, since the mass flow rate declines, the network of them decreases. The exergy of HPP and LPP declines faster than their output network, while the exergy of turbine declines slower than its network. As a result, the exergy of HPP, LPP, and turbine declines when the disturbance occurs. Since the trend of the exergy efficiency of three heat exchangers plays a larger role, the general trend of the system's exergy efficiency reaches the peak first, and then declines. As the decrease of exergy efficiency in HPP, LPP and turbine is larger than the increase in three heat exchangers, the final exergy efficiency of the system is lower than the initial state.

5 CONCLUSION

In this study, a recuperative dual-pressure organic Rankine cycle (RDORC) is adopted. It uses R1234ze(E) as working fluid to recover solid bulk waste heat. In the process of establishing the dynamic model, the finite volume method is adopted. The dynamic parameters of the key components of the system are evaluated under typical step of RDORC heat source inlet temperature T_{hs_01}. The following are the main conclusions:

1.In the case of a step drop of 10°C in the heat source temperature, the exergy efficiency decline mainly occurs in HPP, LPP and turbine. This makes the exergy efficiency of the system drop after the

disturbance. It can be concluded that for the RDORC system, the exergy efficiency of the system under step disturbance can be improved by optimizing the pump and turbine.
2.Exergy efficiency can indicate the efficiency of energy conversion of a system and its components. The research on the exergy efficiency can judge the ability of energy saving, and can also find the most room for improvement. This paper provides a reference for studying the transient response of DORC.

Nomenclature

A	heat transfer area	η	efficiency
c_v	specific heat capacity at constant volume (J/kg K)	τ	time(s)
E	Exergy(kW)	Δx	length of each cell(m)
h	specific enthalpy (J/kg)	α	convective heat transfer coefficient
H	pressure head (m)	ρ	density
HPE	high pressure evaporator	**Subscripts**	
HPP	high pressure pump	che	chemical
I	Exergy loss (kW)	conv	Convective heat transfer
LPE	low pressure evaporator	des	design
LPP	low pressure pump	eva	evaporator
m	mass flow rate (kg/s)	high	high pressure
M	mass of fluid (kg)	hot	hot
N	rotational speed (rpm)	hs_01-hs_03	heat source
ORC	organic Rankine cycle	in	inlet
p	pressure (kPa)	low	low pressure
P	power consumption	out	outlet
q	volumetric flux (m^3/s)	phy	physical
Q	heat transfer rate (W)	pipe	pipe
RDORC	recuperative dual-evaporator ORC	pum	pump
s	specific entropy (J/kg K)	s	isentropic
T	temperature (℃)	tur	turbine
u	specific internal energy (J/kg)	vap	vapor
V	Volume of the discrete cell	w	wall

REFERENCES

Imran, M., et al. (2018). "Recent research trends in organic Rankine cycle technology: A bibliometric approach." Renewable and Sustainable Energy Reviews 81: 552-562.

Lee, C., et al. (2020). "Experimental assessment of convective heat transfer and pressure drop correlation of R1234ze(E) for a supercritical heat exchanger in the organic Rankine cycle." Journal of Mechanical Science and Technology 34(11): 4809-4818.

Kishore, R. A. and S. Priya (2018). "A Review on Low-Grade Thermal Energy Harvesting: Materials, Methods and Devices." Materials (Basel) 11(8).

Wan P., Gong L., Bai Z. (2019). "Thermodynamic analysis of a geothermal-solar flash-binary hybrid power generation system.", Energy Procedia, Volume 158, Pages 3-8,

Zhi, L.-H., et al. (2019). "Thermodynamic analysis of a novel transcritical-subcritical parallel organic Rankine cycle system for engine waste heat recovery." Energy Conversion and Management 197.

Jafary, S., et al. (2020). "A complete energetic and exergetic analysis of a solar powered trigeneration system with two novel organic Rankine cycle (ORC) configurations." Journal of Cleaner Production. Volume 281,124552

Fangyong H., et al. (2020). "Thermodynamic Analysis and Optimization of a Solar-Powered Organic Rankine Cycle with Compound Parabolic Collectors." Journal of Energy Engineering 146(6).

Li, J., et al. (2018). "Parametric optimization and thermodynamic performance comparison of single-pressure and dual-pressure evaporation organic Rankine cycles." Applied Energy 217: 409-421.

Li, J., et al. (2019). "Exergy analysis of novel dual-pressure evaporation organic Rankine cycle using zeotropic mixtures." Energy Conversion and Management 195: 760-769.

Sun, Q., et al. (2020). "Thermodynamic and economic optimization of a double-pressure organic Rankine cycle driven by low-temperature heat source." Renewable Energy 147: 2822-2832.

Lin, S., et al. (2019). "Dynamic performance investigation for two types of ORC system driven by waste heat of automotive internal combustion engine." Energy 169: 958-971.

Manuel J. (2017). "Dynamic study of ORC evaporator operating under fluctuating thermal power from waste heat sources, Energy Procedia." Volume 143, Pages 404-409.

Ni, J., et al. (2018). "Dynamic performance investigation of organic Rankine cycle driven by solar energy under cloudy condition." Energy 147: 122-141.

Chen., et al. (2019). "Dynamic analysis and control strategies of Organic Rankine Cycle system for waste heat recovery using zeotropic mixture as working fluid. ", Energy Conversion and Management 192: 321-334.

Yu., et al. (2021). "Characterization analysis of dynamic behavior of basic ORC under fluctuating heat source", Applied Thermal Engineering 189.